Cross-platform genetic discovery of small molecule products of metabolism and application to clinical outcomes

Luca A. Lotta[1#], Maik Pietzner[1#], Isobel D. Stewart[1], Laura B.L. Wittemans[1,2] ,Chen Li[1], Roberto Bonelli[3,4], Johannes Raffler[5], Emma K. Biggs[6], Clare Oliver-Williams[7,8], Victoria P.W. Auyeung[1], Praveen Surendran[7,9,10,11], Gregory A. Michelotti[12], Robert A. Scott[1], Stephen Burgess[13,14], Verena Zuber[13,15], Eleanor Sanderson[16], Albert Koulman[1,5,17], Fumiaki Imamura[1], Nita G. Forouhi[1], Kay-Tee Khaw[14], MacTel Consortium, Julian L. Griffin[18], Angela M. Wood[7,9,10,19,20,], Gabi Kastenmüller[5], John Danesh[7,9,10,19,21,22,], Adam S. Butterworth[7,9,10,19,21,22], Fiona M. Gribble[6], Frank Reimann[6], Melanie Bahlo[3,4], Eric Fauman[23], Nicholas J. Wareham[1], Claudia Langenberg[1,10*]

 # these authors contributed equally

1) MRC Epidemiology Unit, University of Cambridge, Cambridge, UK
2) The Big Data Institute, Li Ka Shing Centre for Health Information and Discovery, University of Oxford
3) Population Health and Immunity Division, The Walter and Eliza Hall Institute of Medical Research, Parkville, Australia
4) Department of Medical Biology, The University of Melbourne, Parkville, Australia
5) Institute of Computational Biology, Helmholtz Zentrum München – German Research Center for Environmental Health, Neuherberg, Germany
6) Metabolic Research Laboratories, University of Cambridge, Cambridge, United Kingdom
7) British Heart Foundation Cardiovascular Epidemiology Unit, Department of Public Health and Primary Care, University of Cambridge, Cambridge, UK
8) Homerton College, University of Cambridge, Cambridge, UK
9) British Heart Foundation Centre of Research Excellence, University of Cambridge, Cambridge, UK
10) Health Data Research UK Cambridge, Wellcome Genome Campus and University of Cambridge, Cambridge, UK
11) Rutherford Fund Fellow, Department of Public Health and Primary Care, University of Cambridge, UK
12) Metabolon Inc, Durham, North Carolina USA
13) MRC Biostatistics Unit, University of Cambridge, Cambridge, United Kingdom
14) Department of Public Health and Primary Care, University of Cambridge, Cambridge, United Kingdom
15) Department of Epidemiology and Biostatistics, Imperial College London, UK
16) MRC Integrative Epidemiology Unit, Bristol Medical School, University of Bristol, UK
17) NIHR BRC Nutritional Biomarker Laboratory, University of Cambridge, UK
18) Biomolecular Medicine, Department of Metabolism, Digestion and Reproduction, Imperial College London, UK
19) National Institute for Health Research Blood and Transplant Research Unit in Donor Health and Genomics, University of Cambridge, Cambridge, UK
20) The Alan Turing Institute, London, UK
21) National Institute for Health Research Cambridge Biomedical Research Centre, University of Cambridge and Cambridge University Hospitals, Cambridge, UK
22) Department of Human Genetics, Wellcome Sanger Institute, Hinxton, UK
23) Internal Medicine Research Unit, Pfizer Worldwide Research, Cambridge, MA 02142, USA

*Corresponding author:
Claudia Langenberg
MRC Epidemiology Unit
University of Cambridge School of Clinical Medicine
Institute of Metabolic Science
Addenbrooke's Treatment Centre
Cambridge, UK
claudia.langenberg@mrc-epid.cam.ac.uk

Abstract

Circulating levels of small molecules or metabolites are highly heritable, but the impact of genetic differences in metabolism on human health is not well understood. In this cross-platform, genome-wide meta-analysis of 174 metabolite levels across six cohorts including up to 86,507 participants (70% unpublished data), we identify 499 (362 novel) genome-wide significant associations ($p<4.9\times10^{-10}$) at 144 (94 novel) genomic regions. We show that inheritance of blood metabolite levels in the general population is characterized by pleiotropy, allelic heterogeneity, rare and common variants with large effects, non-linear associations, and enrichment for nonsynonymous variation in transporter and enzyme encoding genes. The majority of identified genes are known to be involved in biochemical processes regulating metabolite levels and to cause monogenic inborn errors of metabolism linked to specific metabolites, such as *ASNS* (rs17345286, MAF=0.27) and asparagine levels. We illustrate the influence of metabolite-associated variants on human health including a functional variant (rs17681684) in *GLP2R* associated with citrulline levels, impaired insulin secretion and type 2 diabetes risk. We link genetically-higher serine levels to a 95% reduction in the likelihood of developing macular telangiectasia type 2 [odds ratio (95% confidence interval) per standard deviation higher levels 0.05 (0.03-0.08; $p=9.5\times10^{-30}$)]. We further demonstrate the predictive value of genetic variants identified for serine or glycine levels for this rare and difficult to diagnose degenerative retinal disease [area under the receiver operating characteristic curve: 0.73 (95% confidence interval: 0.70-0.75)], for which low serine availability, through generation of deoxysphingolipids, has recently been shown to be causally relevant. These results show that integration of human genomic variation with circulating small molecule data obtained across different measurement platforms enables efficient discovery of genetic regulators of human metabolism and translation into clinical insights.

Introduction

Metabolites are small molecules that reflect biological processes and are widely measured in clinical medicine as diagnostic, prognostic or treatment response biomarkers[1]. Blood levels of metabolites are highly heritable as shown by previous studies which attempted to characterise the genetic architecture of metabolite variation in the general population [2,3,4,5,6,7,8]. Previous studies have been limited in scope by a focus on metabolites assessed using a single method. Integration of genetic association results for metabolites measured on different platforms can help maximise the power for a given metabolite and provide a more refined understanding of genetic influences on blood metabolite levels and human physiology.

To identify genomic regions regulating metabolite levels and systematically study their relevance for disease, we conducted a cross-platform meta-analysis of genetic effects on levels of 174 blood metabolites measured in large-scale population-based studies on the Biocrates (AbsoluteIDQ™ p180, Fenland Study), Nightingale (^{1}H-NMR, Interval Study) or Metabolon (Discovery HD4™, EPIC-Norfolk and Interval Studies) platforms combined with previously reported results [9104]. We launch with this publication a webserver to easily query our results for the purpose of targeted genetic studies, such as Mendelian randomization.

Results

Associations with blood metabolites at 144 genomic regions

Genome-wide meta-analyses were conducted for 174 metabolites from 7 biochemical classes (i.e. amino acids, biogenic amines, acylcarnitines, lyso-phosphatidylcholines, phosphatidylcholines, sphingomyelins and hexose) commonly measured using the Biocrates p180 kit in up to 86,507 individuals, contributing over 3.7 million individual-metabolite data points (70% from unpublished studies; **Fig. 1**). For each of the 174 metabolites, this was the largest genome-wide association analyses (GWAS) to date, with at least a doubling of sample size (**Fig. 1C**). Sample sizes ranged from 8,569 to 86,507 individuals for metabolites depending on the platform used in each contributing study. Using GWAS analyses we estimated the association of up to 10.2 million single nucleotide variants with a minor allele frequency (MAF) >0.5%, including 6.1 million with MAF ≥ 5%.

We identified 499 variant-metabolite associations (362 novel) from 144 loci (94 novel) at a metabolome-adjusted genome-wide significance threshold of $p<4.9\times10^{-10}$ (correcting the usual GWAS-threshold, $p<5\times10^{-8}$, for 102 principle components explaining 95% of the variance in metabolite levels using principle component analysis; **Fig. 1**). The vast majority of these associations

were consistent across studies and measurement platforms [median I^2: 26.8 (interquartile range: 0 – 70.1) for 465 associations with at least two contributing studies] (**Supplementary Tables 1-2**). To identify possible sources of heterogeneity, we investigated the influence of differences by cohort, measurement platform, metabolite class, and association strength in a joint meta-regression model (**Supplementary Table 3**). This showed that heterogeneity was mainly due to the overall strength of the signal, i.e. associations with higher z-scores showed greater heterogeneity ($p<1.05x10^{-9}$). However, the majority of these statistically heterogeneous associations were directional consistent and nominally significant across and within each strata for 146 of 170 associations with a z-score > 10, demonstrating the feasibility of pooling association estimates across metabolomics platforms for the purpose of genetic discovery. Genetic variants at the *NLRP12* locus, e.g. rs4632248, were a notable exception with large estimates of heterogeneity (I^2>90%). The *NLRP12* locus is known to affect the monocyte count[11] and has been shown to have pleiotropic effects on the plasma proteome in the INTERVAL study[12]. Monocytes, or at least a subpopulation subsumed under this cell count measure, release a wide variety of biomolecules upon activation or may die during the sample handling process and hence releasing intracellular biomolecules, such as taurine[13], into the plasma. In brief, one specific source of heterogeneity in mGWAS associations might relate to sample handling differences across studies.

This highlights the utility of our genetic cross-platform approach to maximise power for a given metabolite, substantially extending previous efforts for any given metabolite[14]. Previously reported associations from platform-specific studies were also found to generally be consistent in our cross-platform meta-analysis (**Supplementary table 2; *webserver link to be inserted***).

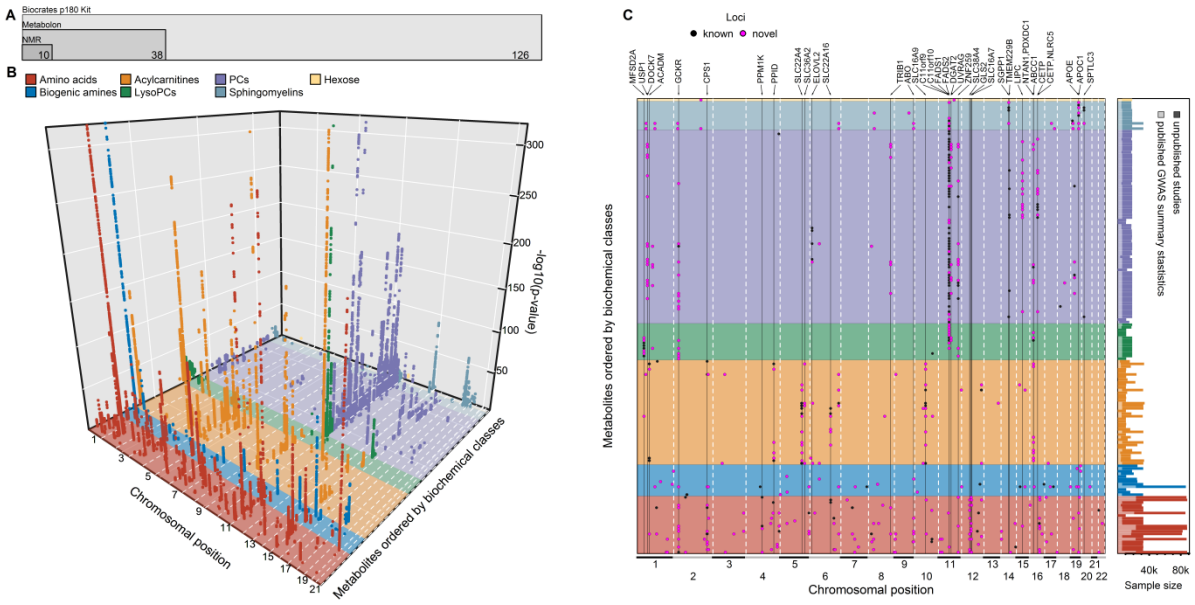

Figure 1A Overlap among the 174 plasma metabolites investigated in the present study across three different techniques: Biocrates p180 Kit, Metabolon HD4, and proton nuclear magnetic resonance spectroscopy (NMR). **B** A three-dimensional Manhattan plot displaying chromosomal position (x-axis) of significant associations ($p < 4.9 \times 10^{-10}$, z-axis) across all metabolites (y-axis). Colours indicate metabolite groups. **C** A top view of the 3D-Manhattan plot. Dots indicate significantly associated loci. Colours indicate novelty of metabolite – locus associations. Loci with indication for pleiotropy have been annotated. Barplot on the right-hand side indicates samples sizes for each metabolite comparing the present samples sizes with the previous largest genome-wide association study for a specific metabolite. PCs = phoshpatidylcholines, LysoPCs = lysophophatidylcholines

Insights in the genetic architecture of metabolite levels

We found a median of 2 (range: 1-67, **Fig. 2A**) associated metabolites for each locus and a median of 3 (range: 1-20, **Fig. 2B**) locus associations for each metabolite, reflecting pleiotropy and the extensive contribution of genetic loci to circulating metabolite levels. The number of associations was proportional to the estimated heritability and the sample size of the meta-analysis for a given trait (**Fig. 2C**).

Similar to what is routinely observed in GWAS literature, effect size estimates increased with decreasing minor allele frequency (MAF) (**Fig. 3A**). However, there were 26 associations (**Supplemental Table 2**) for common lead variants with per-allele differences in metabolites levels greater than 0.25 standard deviations (SD), a per-allele effect size that is >3-fold larger than the strongest common variants associated with SDs of body mass index at the *FTO* locus.

Variants identified in this study explained up to 23% of the variance (median: 1.4%; interquartile range: 0.5% - 2.8%) and up to 99.8% of the chip-based heritability (median 9.2%; interquartile range: 4.7% - 17.1%) for the 141 metabolites with at least one genetic association (**Fig. 2D**). The 26 common variants with large effect sizes (>0.25 SD per allele) were identified for metabolites with higher heritability (**Fig. 2D**) and accounted for up to 74% of the heritability explained in those metabolites.

GWAS analyses generally assume a linear relationship between genotypes and phenotypes, i.e. an additive dose-response model. The identification of several metabolite-associated variants with large effect sizes and availability of individual-level data in the Fenland cohort allowed us to test whether the metabolite-associated variants showed evidence of deviation from a linear model. Of 499 associations tested, 9 showed evidence of departure from a linear association ($p<0.0001$; 180-fold more than expected by chance; two-tailed binomial $p<2.2\times10^{-16}$; **Fig. 2E-M**). Modelling actual genotypes rather than assuming linear associations in these instances explained a median of 7.4% more (range: 1.4-15.2%) of the heritability in metabolite levels (**Fig. 2N**).

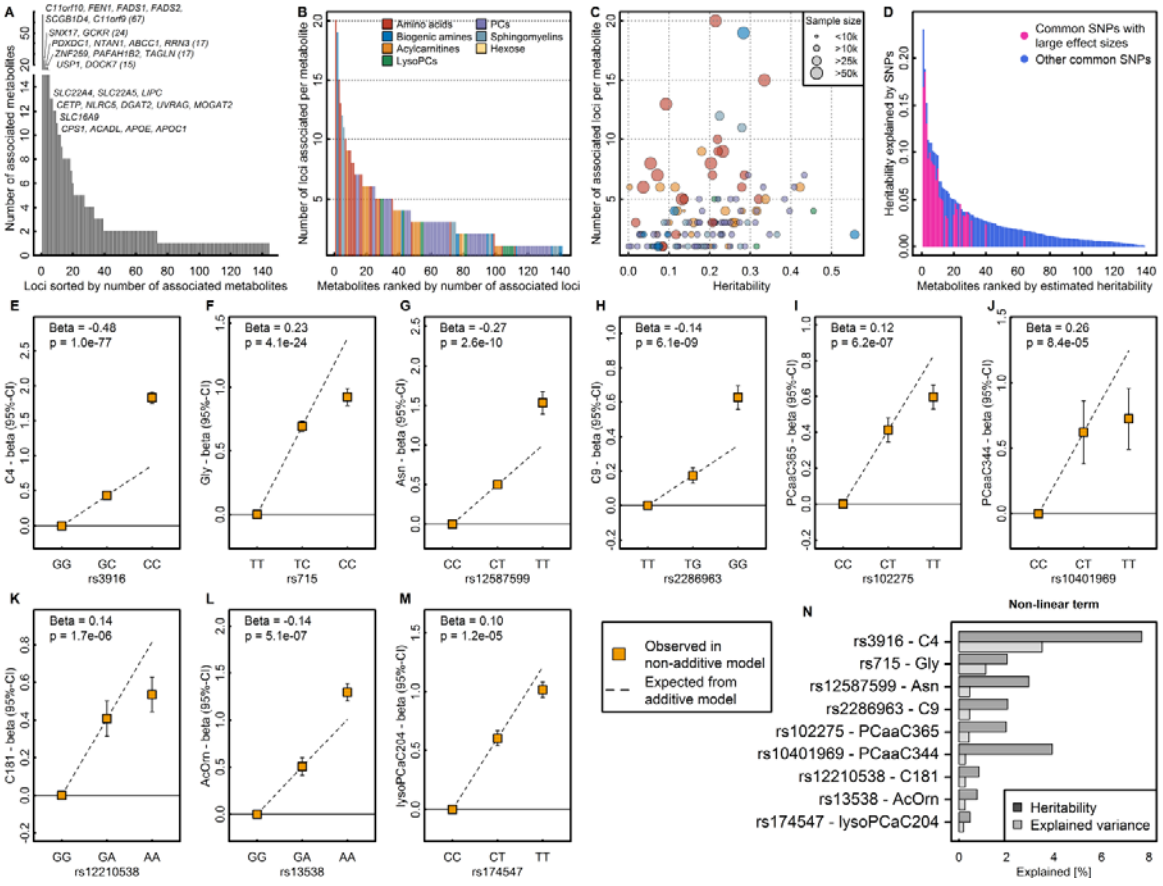

Figure 2A Distribution of pleiotropy, i.e. number of associated metabolites, among loci identified in the present study. **B** Distribution of polygenicity of metabolites, i.e. number of identified loci for each metabolite under investigation. **C** Scatterplot comparing the estimated heritability of each metabolite against the number of associated loci. Size of the dots indicates samples sizes. **D** Heritability estimates for single metabolites. Colours indicate the proportion of heritability attributed to single nucleotide polymorphisms (SNPs) with large effect sizes (β>0.25 per allele). **E – M** SNP – metabolite association with indication of non-additive effects. Beta is an estimate from the departure of linearity. **N** Barplot showing the increase in heritability and explained variance for each SNP – metabolite pair when including non-additive effects.

In 61 of the 499 associations the lead association signal was a nonsynonymous variant, a 40-fold enrichment compared to what would be expected by chance given the annotation of ascertained genetic variants (two-tailed binomial test, $p=5\times10^{-30}$, **Fig. 3D**). For a further 59 associations, the lead variant was in high LD with a nonsynonymous variant ($R^2>0.8$). Lead variants that were nonsynonymous, or variants in high LD with a nonsynonymous variant, generally had lower MAF and larger effect sizes than variants that were not in these categories (**Fig 3B-C**).

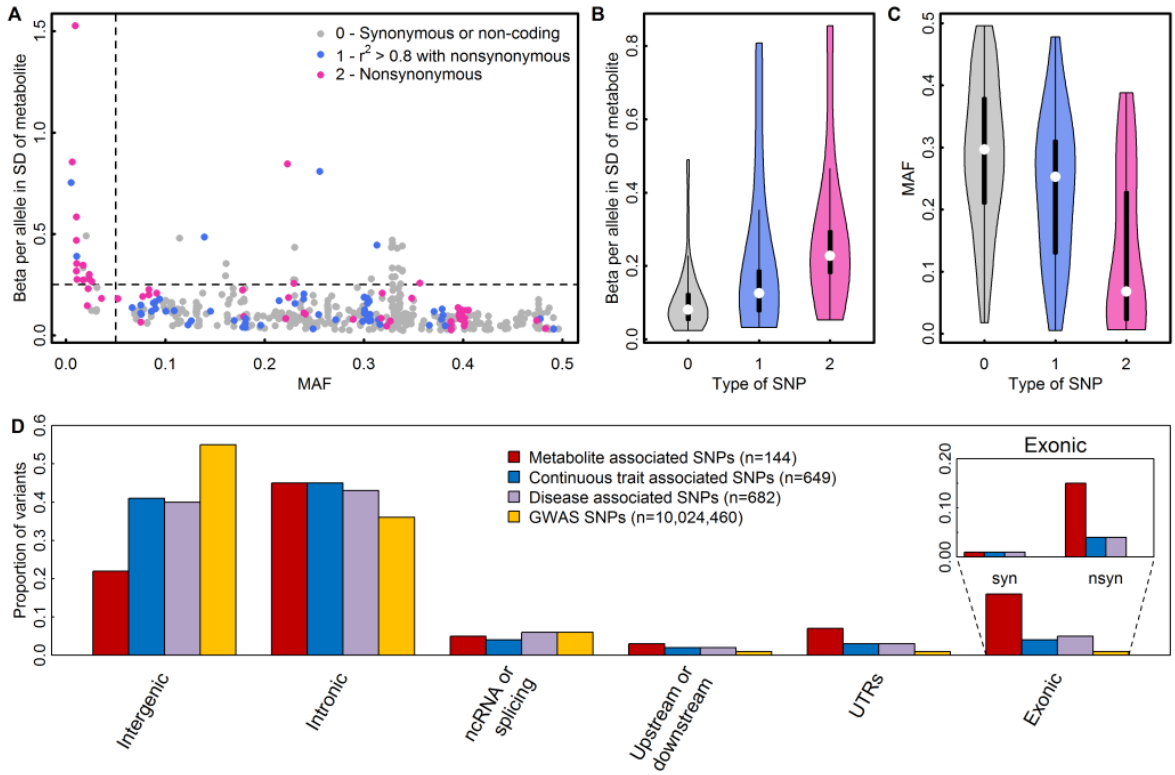

Figure 3A Scatterplot comparing the minor allele frequencies (MAF) of associated variants with effect estimates from linear regression models (N loci=499). Colours indicate possible functional consequences of each variant: maroon – nonsynonymous variant; blue – in strong LD ($r^2>0.8$) with a nonsynonymous variant and grey otherwise. **B/C** Distribution of effect sizes (B) and allele frequencies (C) based on the type of single nucleotide polymorphism (SNP) (0 – non-coding or synonymous, 1 – in strong LD with nonsynonymous, 2 - nonsynonymous). **D** Distribution of functional annotations of metabolite associated variants (red), trait-associated variants (blue – continuous, purple – diseases) obtained from the GWAS catalogue, and all SNPs included in the present genome-wide association studies. The inlet for exonic variants distinguishes between synonymous (syn) and nonsynonymous variants (nsyn).

We identified 22 loci harbouring two (n=21) or three (n=1) independent signals, i.e. different plasma metabolites were associated with distinct genetic variants within the same genomic region (**Supplementary Table S2**). For six regions our two different annotations approaches assigned only one causal gene (see below and **Methods**), including *ACADM*, *GLDC*, *ARG1*, *MARCH8*, *SLC7A2*, and *LIPC* (**Supplementary Table S2**). We found evidence that allelic heterogeneity, i.e. conditionally independent variants at a locus for a specific metabolite, explains the association pattern at 3 of those loci (*ACADM*, *ARG1*, and *LIPC*; **Supplementary Table S4**). We identified another 16 loci

harbouring at least one (range: 2–6) additional conditionally independent variant(s) in exact conditional analyses (see **Methods**, **Supplementary Table S4**).

Effector genes, tissues, pathways

We used two complementary strategies to prioritize likely causal genes for the observed associations: (1) a hypothesis-free genetic approach based on physical distance, genomic annotation and integration of expression quantitative trait loci (eQTLs) to prioritize genes in a systematic and standardised way (see **Methods**), and (2) a biological knowledge-based approach integrating existing knowledge about specific metabolites or related pathways to identify biologically plausible candidate genes from the 20 genes closest to the lead variant (**Fig. 4A**). Using the hypothesis-free genetic approach, we identified 249 unique likely causal genes for the 499 associations, with at least one gene per association and some genes prioritized as likely causal for multiple metabolite associations. The knowledge-based approach identified 130 biologically plausible genes for 349 out of 499 associations. We asked whether the hypothesis-free genetic approach identified biologically plausible genes (prioritized by strategy 2) more often than expected by chance. An excess of biologically plausible genes amongst those prioritized by the hypothesis-free genetic algorithm would suggest that the approach is able to prioritize true positive associations that map to known pathways or underlying biology. Amongst 9,980 genes screened at the 499 associations, 420 (4.2%) were biologically plausible. A total of 350 gene-metabolite assignments from the first approach were also annotated in the knowledge-based approach with 126 pairs (36%) termed biologically plausible (~8-fold more than expected by chance; two-tailed binomial test, $p=2.3\times10^{-80}$; **Fig. 4B**). Among the consistently assigned genes between both approaches assignment of the nearest gene (124 times out of 126, X^2-test, $p<2.5\times10^{-45}$) was the strongest shared factor, as might be expected, followed by presence of a missense variant at least in LD ($R^2>0.8$, 30 times out of 126, X^2-test, $p<1.3\times10^{-07}$) and only a minor contribution of eQTL data (20 times out of 126, X^2-test, $p<0.001$). Over 70% of genetically prioritized genes were enzymes or transporters (**Fig. 4C**).

In addition to being enriched in genes previously implicated in the biology of these metabolites, the genetically prioritized genes were also enriched in genes known for mutations to cause rare inborn errors of metabolism (IEMs), i.e. monogenic defects in the metabolism of small molecules with very specific metabolite changes (**Fig. 4B**).

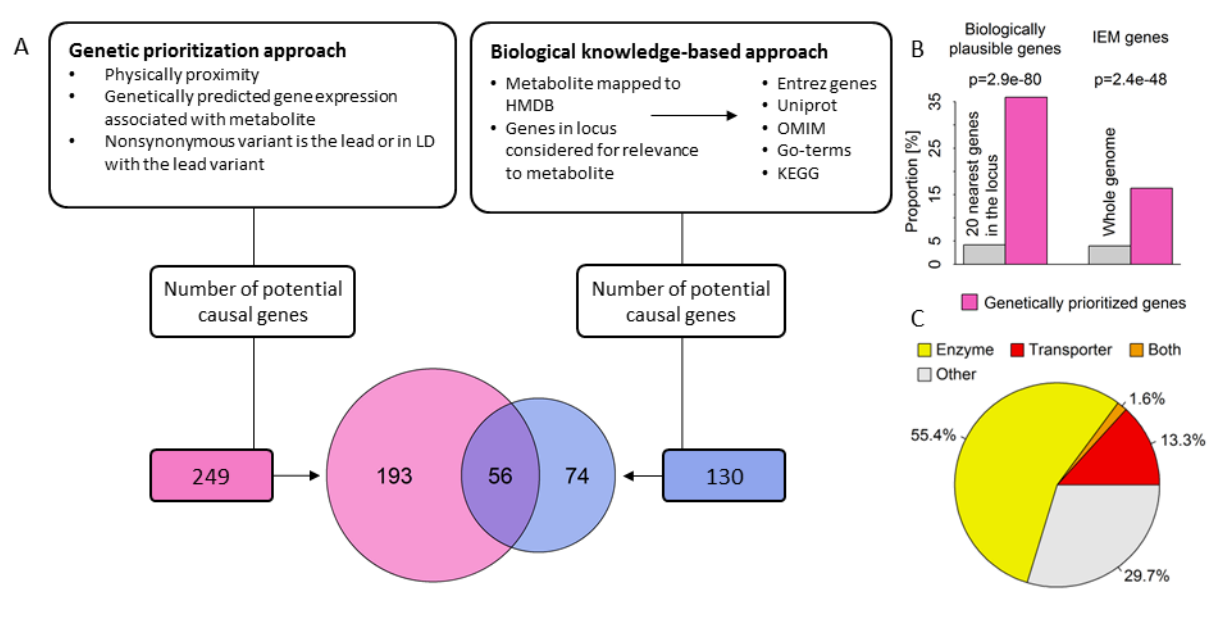

Figure 4A Comparison between the hypothesis-free genetically prioritized versus biologically plausible approaches used in the present study to assign candidate genes to metabolite associated single nucleotide polymorphisms. The Venn-diagram displays the overlap between both approaches. **B** Enrichment of genetically prioritized genes among biologically plausible or genes linked to inborn errors of metabolism (IEM). **C** Proportion of genetically prioritized genes encoding for either enzymes or transporters.

Integrating GWAS statistics across cohorts and platforms allowed us to identify three genes that have never been associated with any metabolite level so far. At the *CERS6* locus, rs4143279 associates with levels of sphingomyelin (d18:1/16:0)) ($p = 4.2x10^{-10}$). *CERS6* encodes a ceramide synthase facilitating formation of ceramide, a precursor of sphingomyelins[15]. At the *ASNS* locus, rs17345286 associates with levels of asparagine ($p = 4.7x10^{-20}$). The lead variant is in high LD ($R^2=1$) with a missense mutation in *ASNS* (rs1049674, p.Val210Glu). *ASNS* encodes an asparagine synthase[16]. Finally, at the *SLC43A1* locus, rs2649667 associates with levels of phenylalanine ($p = 3.6x10^{-13}$). *SLC43A1* encodes a liver-enriched transporter of large neutral amino acids, including phenylalanine[17].

Insights into the causes of common and rare diseases from metabolite-associated loci

The phenotypic consequences of metabolite-associated variants are currently not well characterized. Here, we systematically investigate the contribution of individual loci and polygenic predisposition associated with differences in metabolite levels to the risk of common and rare diseases.

A citrulline-raising functional variant in GLP2R increases type 2 diabetes risk

Because several of the metabolites captured in this GWAS have been associated with incident type 2 diabetes, we sought to investigate whether the association between metabolite-associated

loci and diabetes could provide insights into underlying pathophysiologic mechanisms. Using estimates of effect for association with type 2 diabetes based on a meta-analysis of 80,983 cases and 842,909 controls (see **Methods**), we observed a significant enrichment for associations with type 2 diabetes (p-value=$2.8x10^{-7}$) of metabolite-associated variants compared to a matched control set of variants (**Fig. 5A**).

Amongst the diabetes- and metabolite-associated loci was a missense p.Asp470Asn (rs17681684) variant in the *GLP2R* gene encoding the receptor for glucagon-like peptide 2, a 33 amino acid peptide hormone encoded by the proglucagon gene (*GCG*) that stimulates the growth of intestinal tissue. Common variants at *GLP2R* are associated with an increased risk of type 2 diabetes (T2D) and lower levels of insulin secretion[18]. The previously reported lead variant for T2D (rs78761021) is in high LD (0.87) with our lead citrulline association signal at GLP2R (rs17681684), which was associated with a 4% higher type 2 diabetes risk (per-allele odds ratio, 1.04; 95% confidence interval, 1.02, 1.05; p=1.1×10^{-08}), comparable to previous reports[18]. Our results show that the genetic signal for association with T2D statistically colocalises (posterior probability=0.94) with that for citrulline (**Fig. 5B**), levels of which reflect the volume of intestinal cells and are a marker of GLP2R target engagement in the treatment of short-bowel syndrome with glucagon-like peptide 2 analogues[19]. The *GLP2R* p.Asp470Asn variant was the only of 6 independent genome-wide significant citrulline-raising loci that was associated with a higher risk of type 2 diabetes, which indicates that the association does not reflect a general impact of citrulline levels on diabetes risk but rather a locus-specific association at *GLP2R* (**Fig. 5C**). Taken together, this suggests that genetically higher GLP2R signalling, indicated by the higher citrulline levels among *GLP2R* 470Asn carriers, is associated with an increased risk of diabetes via lower insulin secretion.

G-protein coupled receptors like GLP2R may signal via G-protein-dependent cyclic adenosine monophosphate (cAMP) production or via G-protein-independent beta-arrestin mediated signalling[20]. To investigate if the *GLP2R* p.Asp470Asn variant affects signalling via either of these pathways, we expressed the *GLP2R* p.Asp470Asn variant in different *in vitro* models (see **Methods**). We show that the variant allele is significantly associated with reduced recruitment of beta-arrestin to GLP2R upon glucagon-like peptide 2 stimulation, but not with cAMP signalling, which suggests a potential role for impaired beta-arrestin recruitment to GLP2R in the pathophysiology of type 2 diabetes (**Fig. 5D-F**).

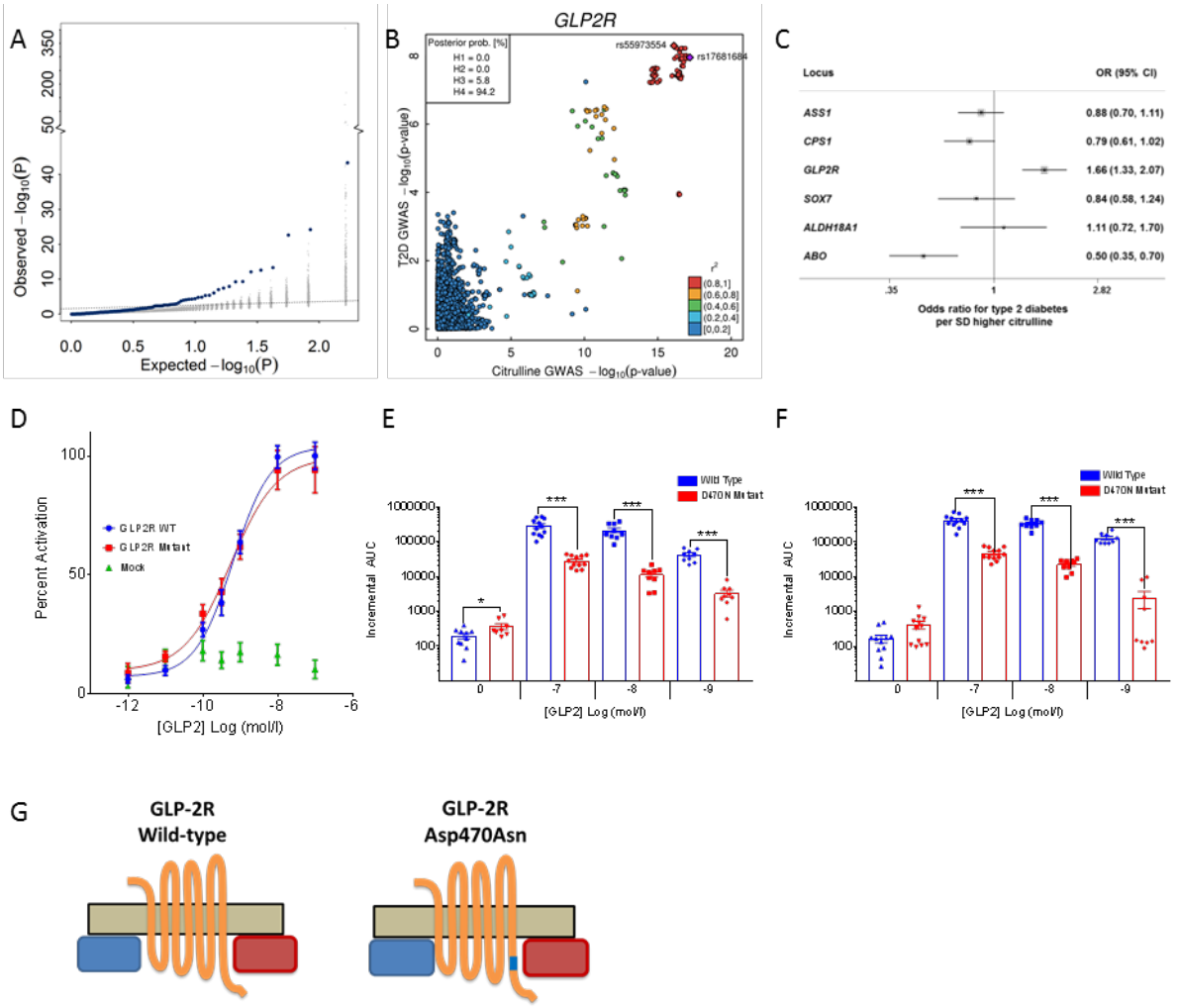

Figure 5A Enrichment of associations with type 2 diabetes (T2D: 80,983 cases, 842,909 controls) among metabolite-associated SNPs. Blue dots indicate metabolite-SNPs and grey dots indicate a random selection of matched control SNPs. **B** Opposing $-\log_{10}$(p-values) from the genome-wide association study of plasma citrulline with those from the T2D-GWAS for SNPs located around *GLP2R*. The legend in the upper left gives the posterior probabilities (PP) from statistical colocalisation analysis. H4 = PP for the hypothesis of a shared causal variant. **C** Individual association summary statistics for all citrulline associated SNPs (coded by the citrulline increasing allele) for T2D. **D** GLP-2 dose response curves in cAMP assay for GLP2R wild-type and mutant receptors. The dose response curves of cAMP stimulation by GLP-2 in CHO K1 cells transiently transfected with either GLP2R wild-type or mutant constructs. Data were normalised to the wild-type maximal and minimal response, with 100% being GLP-2 maximal stimulation of the wild-type GLP2R, and 0% being wild-type GLP2R cells with buffer only. Mean ± standard errors are presented (n=4).**E-F** Summary of wild-type and mutant GLP2R beta-arrestin 1 and beta-arrestin 2 responses. Area under the curve (AUC) summary data (n=3-4) displayed for beta-arrestin 1 recruitment (E) and beta-arrestin 2 recruitment (F). AUCs were calculated using the 5 minutes prior to ligand addition as the baseline value. Mean ± standard errors are presented. Normal distribution of log10 transformed data was determined by the D'Agostino & Pearson normality test. Following this statistical significance was assessed by one-way ANOVA with post hoc Bonferroni test. ***p<0.001, *p<0.05. **G** Schematic sketch for the location of the missense variant induces amino acid substitution in the glucagon-like peptide-2 receptor (GLP2R).

Serine and glycine levels play a critical role in the aetiology of a rare eye disease

A recent GWAS of macular telangiectasia type 2 (MacTel), a rare neurovascular degenerative retinal disease, identified three genome-wide susceptibility loci (*PHGDH*, *CPS1*, and *TMEM161B–LINC00461*) of which the same variants at *PHGDH* and *CPS1* were associated with levels of the amino acids serine and glycine in this GWAS[21]. More recently, it was shown that low serine availability is

linked to both MacTel as well as hereditary sensory and autonomic neuropathy type 1 through elevated levels of atypical deoxyshingolipids[22]. Whether genetic predisposition to low serine and glycine levels affects MacTel more generally or has predictive utility has not been investigated. To test this and to explore the specificity of associations between genetic influences on metabolite levels and the risk of MacTel, we generated genetic risk scores (GRS) using the sentinel variants for each of the 141 metabolites with at least one significantly associated locus identified in this GWAS and tested their associations with the risk of MacTel. GRS's for serine and glycine were the only scores associated with risk for MacTel after removal of the known highly pleiotropic *GCKR* variant (**Fig. 6A**). Each standard deviation higher serine levels via the serine GRS was associated with a 95% lower risk of MacTel (odds ratio (95% confidence interval), 0.05 (0.03-0.08); $p=9.5\times10^{-30}$; **Fig. 6A**). Each of five serine associated variants was individually associated with lower MacTel risk, with a clear dose-response relationship and no evidence of heterogeneity (**Fig. 6B**). The association was unchanged when removing the *GCKR* locus. To disentangle the effect of these two highly correlated metabolites on MacTel risk, we used multivariable Mendelian randomization analysis, which allowed us to test for a causal effect of both measures simultaneously. In this analysis, the effect of serine remained strong, while the effect of glycine was attenuated (**Tab. 1**). Glycine and serine can be interconverted and these results provide genetic evidence that the link between glycine and MacTel is via serine levels through glycine conversion. This hypothesis is supported by the evidence of a log-linear relationship between associations with serine and risk of MacTel among glycine-associated variants (**Fig. 6B**). These findings provide strong evidence that pathways indexed by genetically higher serine levels are strongly and causally associated with protection against MacTel.

Given the large observed effect size, we estimated whether using serine and glycine-associated loci might improve the prediction of this rare disease. Adding genetically predicted glycine and serine levels substantially improved prediction of MacTel based on an area under the receiver operating characteristic curve from 0.65 (CI 95%: 0.626-0.682) to 0.73 (0.702-0.753) (**Fig. 6**).

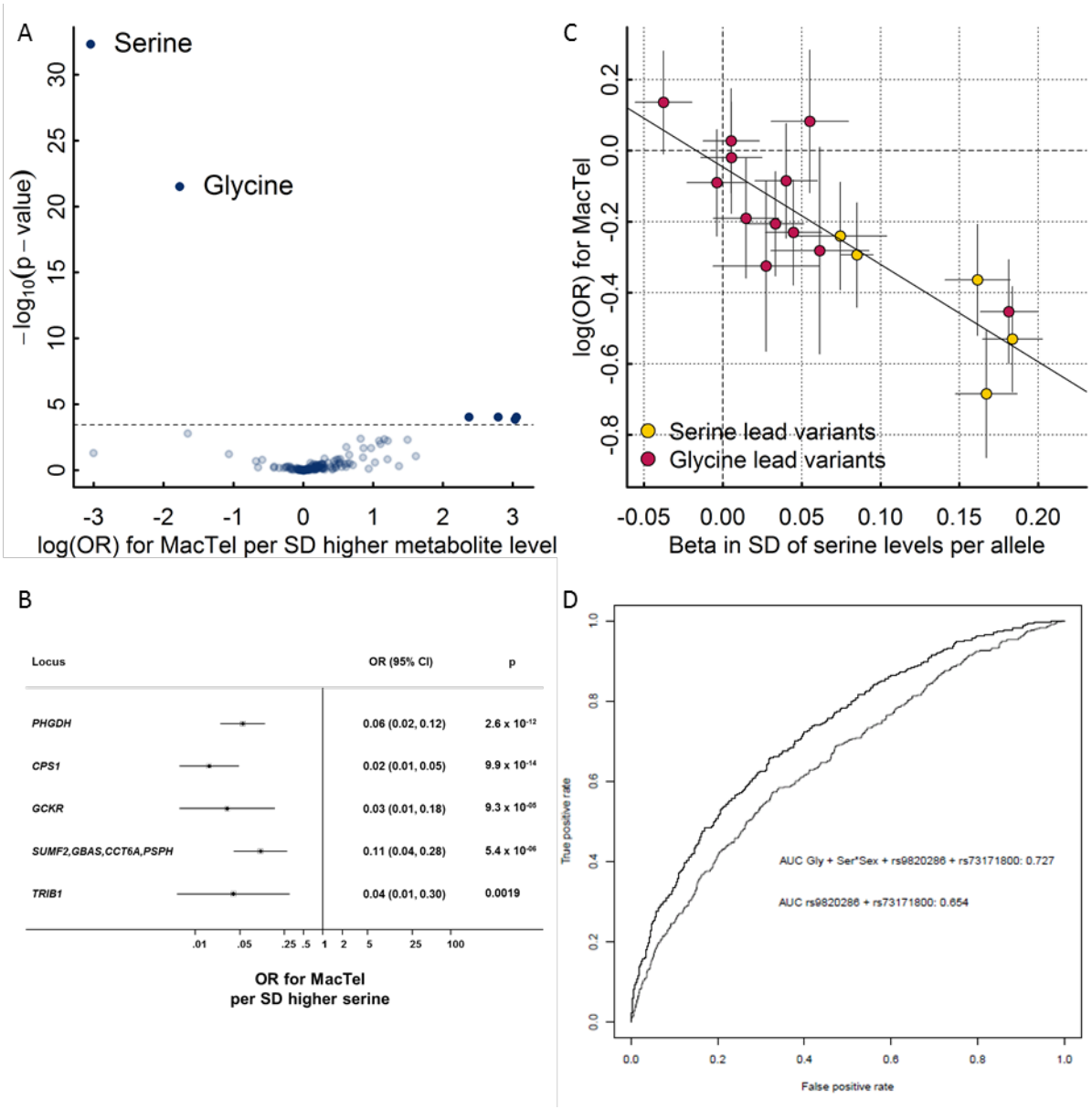

Figure 6A Results from polygenic risk scores (PGS) for each metabolite on risk for macular telangiectasia type 2 (MacTel). The dotted line indicates the level of significance after correction for multiple testing. The inlet shows the same results but after dropping the pleiotropic variants in *GCKR* and *FADS1-2*. **B** Effect estimates of serine-associated genetic variants on the risk for MacTel. **C** Comparison of effect sizes for lead variants associated with plasma serine levels and the risk for MacTel. **D** Receiver operating characteristic curves (ROC) comparing the discriminative performance for MacTel using a) sex, the first genetic principal component, and two MacTel varaints (rs73171800 and rs9820286) not associated with metabolite levels, and b) additionally including genetically predicted serine and glycine at individual levels as described in the methods. The area under the curve (AUC) is given in the legend.

Common variation at inborn error of metabolism (IEM) associated genes influences the risk of common manifestations of diseases related to the phenotypic presentation of those IEMs

In his seminal 1902 work on alkaptonuria[23], also known as dark or black urine disease, Archibald Garrod was the first to hypothesise that inborn errors of metabolism are “extreme examples of variations of chemical behaviour which are probably everywhere present in minor degrees”. Previous studies have shown enrichment of metabolite quantitative trait loci in genes known to

cause IEMs[9]. Whether or not these differences translate into clinically manifest disease remains unknown. The identification of several metabolite-associated variants at IEM-linked genes in this GWAS meta-analysis allows an investigation of the health consequences of genetically determined differences in metabolism for more frequently occurring variants, representing potentially milder forms of the metabolic and other clinical symptoms of IEMs, and providing new candidate genes for rare extreme metabolic disorders that currently lack a genetic basis (**Fig. 7A**). In this study, there were 153 locus-metabolite associations for which 53 unique IEM-associated genes were prioritized as likely causal using either the hypothesis-free genetic approach or the knowledge-based approach on the basis of the Orphanet database[24]. In 89% of these associations (136 of 153) the metabolite associated with a given GWAS locus perfectly matched, or was closely related to, the metabolite affected in patients with the corresponding IEM (**Fig. 7B**).

To test whether IEM-mirroring lead variants from our metabolite GWAS may increase the risk of common manifestations of diseases known to exist in patients with the corresponding IEM (**Fig. 7A**) we obtained a list of electronic health record diagnosis codes (International Statistical Classification of Diseases and Related Health Problems 10th Revision [ICD-10]) and mapped those based on symptoms seen in both, IEM patients and patients with common, complex disease manifestations (see **Methods**). We identified 93 ICD-10 codes with at least 500 cases within the UK Biobank study which aligned with the symptomatic seen in IEMs caused by mutations in genes associated with metabolite levels in the present study. We obtained the association statistics of 85 unique metabolite-associated lead variants at the 136 locus-metabolite associations with these 93 clinical diagnoses and observed 36 associations that met statistical significance (false discovery rate < 5%, **Supplemental Table S5 and Fig. 7B**). For 15 out of those we obtained strong evidence of a shared genetic metabolite-phenotype signal using colocalisation analyses (posterior probability of a shared signal >80%; **Fig. 7D and Supplemental Fig. S1**). These instances linked common genetic variants in or near *APOE*, *PCSK9, LPL,* and *LDLR* associated with sphingomyelins (SM 16:0, SM 18:0, and SM-OH 24:1) with atherosclerotic heart disease diagnosis codes (I21, I25), mirroring what is observed in rare familial forms of dyslipidaemia in which these sphingomyelins are elevated and the risk of ischemic heart disease is greatly increased[25,26]. These results provide further evidence that common variation at IEM genes can lead to clinical phenotypes and diseases that correspond to those that patients with rare mutations in those same genes are severely affected by. Further studies with detailed follow-up for specific outcomes may provide greater power and help clarify the medical consequences of genetic differences in metabolism caused by metabolite altering variants in the general population.

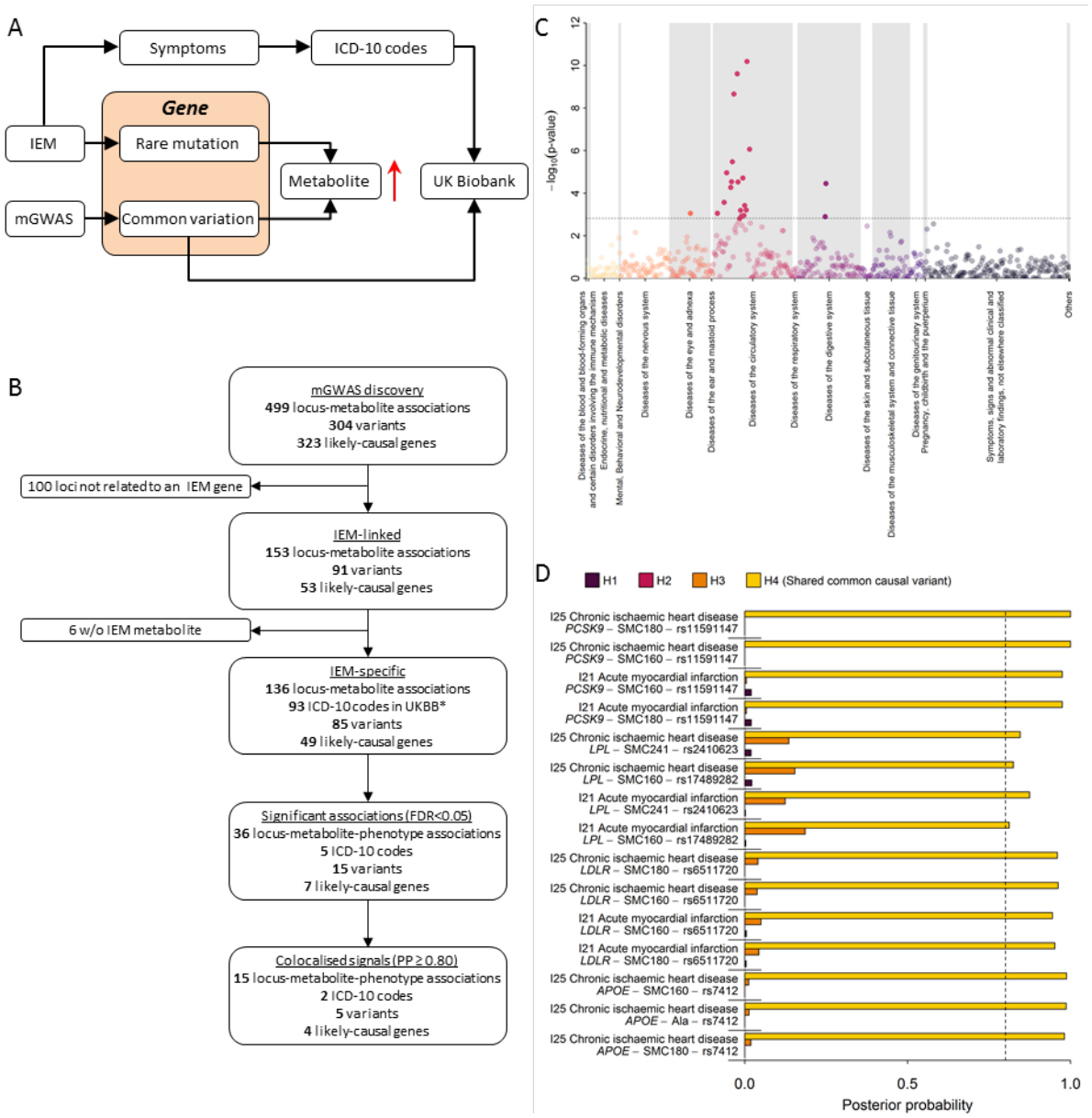

Figure 7A Scheme of the workflow to link common variation in genes causing inborn errors of metabolism (IEM) to complex diseases. **7B** Flowchart for the systematic identification of metabolite-associated variants to genes and diseases related to inborn errors of metabolism (IEM). **C** P-values from phenome-wide association studies among UK Biobank using variants mapping to genes knowing to cause IEMs and binary outcomes classified with the ICD-10 code. Colours indicate disease classes. The dotted line indicates the significance threshold controlling the false discovery rate at 5%. **D** Posterior probabilities (PPs) from statistical colocalisation analysis for each significant triplet consisting of a metabolite, a variant, and a ICD-10 code among UK Biobank. The dotted line indicates high likelihood (>80%) for one of the four hypothesis tested: H0 – no signal; H1 – signal unique to the metabolite; H2 – signal unique to the trait; H3 – two distinct causal variants in the same locus and H4 – presence of a shared causal variant between a metabolite and a given trait.

Discussion

This large-scale genome-wide meta-analysis has integrated genetic associations for 174 metabolites across different measurement platforms, an approach that has resulted in a three-fold increase in our knowledge of genetic loci regulating levels of these metabolites. We assign likely

causal genes for many of the identified associations using a dual approach that combined automated database mining with manual curation.

Previous platform-specific genetic studies of blood metabolites have been substantially smaller in size due to being restricted to a single platform and/ or study[2,3,4,5,6,7,8]. We build on these earlier studies to identify and demonstrate enrichment of rare and low-frequency coding variants in enzyme and transporter genes with large effects and reveal the importance of non-linear associations at several loci.

Our results not only provide detailed insight into the genetic determinants of human metabolism but consider their relevance for disease aetiology and prediction. We explore both locus-specific and polygenic score effects and provide tangible examples with clear translational potential. We discovered a strong link between GLP2R, citrulline metabolism and type 2 diabetes, and demonstrate that the p.Asp470Asn variant underlying the citrulline and diabetes associations leads to significantly reduced recruitment of beta-arrestin to GLP2R in various cellular models. GLP2R is related to GLP1R, a target of glucose-lowering therapeutic agonists approved for type 2 diabetes that mimic the other proglucagon gene encoded peptide glucagon-like peptide 1.

The finding that a standard deviation increase in serine levels via a genetic risk score is associated with 95% lower risk of MacTel shows that genetic differences resulting in very specific metabolic consequences can have profound effects on health. Our results suggest that inclusion of genetic scores for metabolite levels can improve identification of high risk individuals. Serine and glycine supplementation and/ or pharmacologic modulation of serine metabolism may help to reduce development or alter the prognosis of this rare, severe eye disease, specifically if targeted to people genetically with a genetic susceptibility to low serine levels. It is important to note, that randomized control trials are needed testing this hypothesis before any recommendations on supplementations could be made.

We finally show specific examples where common genetic variation in IEM-related genes is associated with phenotypes that are also caused by rare highly penetrant mutations. These results suggest that rare variants in metabolite regulating genes newly identified in our study may be valuable candidate genes in patients without a genetic diagnosis but severe alterations in the corresponding or related metabolites. Hence these results provide a new starting point for further investigations into the relationships between human metabolism and common and rare disorders.

Methods

Study design and participating cohorts

We performed genome-wide meta-analyses of the levels of 174 metabolites from 7 biochemical categories (amino acids, biogenic amines, acylcarnitines, phosphatidylcholines, lysophosphatidylcholines, sphingomyelins, and sum of hexoses) captured by the Biocrates p180 kit measured using mass spectrometry (MS). As described in more detail below, a total of 174 metabolites were successfully measured in up to 9,363 plasma samples from genotyped participants of the Fenland study [27].

To maximise sample size and power, we meta-analysed genome-wide association (GWAS) results from the Fenland cohort with those run in the EPIC-Norfolk [28] and INTERVAL [29] studies, in which metabolites were profiled using MS (Metabolon Discovery HD4 platform) or protein nuclear magnetic resonance (^{1}H-NMR) spectrometry [3031] (**Supplementary Table 1**). Ten of the 174 Biocrates metabolites were covered across all platforms, while 38 were available on the Biocrates and Metabolon platforms and 126 were unique to Biocrates (**Fig. 1**). We integrated publicly available summary statistics from genome-wide meta-analyses of the same metabolites measured using MS (with Biocrates or Metabolon platforms) or ^{1}H-NMR spectrometry (**Supplementary Table 1**). Metabolites were matched across platforms by comparing metabolite names and biochemical formulas. Mapping across different Metabolon platforms was done based on retention time/index (RI), mass to charge ratio (m/z), and chromatographic data (including MS/MS spectral data). Scientists at Metabolon Inc. independently reviewed and confirmed metabolite matches.

A summary of the characteristics of participating cohorts is given in **Supplemental Table S1**. The Fenland study is a population-based cohort study of 12,435 participants without diabetes born between 1950 and 1975 [27]. Participants were recruited from general practice surgeries in Cambridge, Ely and Wisbech (United Kingdom) and underwent detailed metabolic phenotyping and genome-wide genotyping. The European Prospective Investigation of Cancer (EPIC)-Norfolk study is a prospective cohort of 25,639 individuals aged between 40 and 79 and living in the county of Norfolk in the United Kingdom at recruitment [28]. INTERVAL is a randomised trial of approximately 50,000 whole blood donors enrolled from all 25 static centres of NHS Blood and Transplant, aiming to determine whether donation intervals can be safely and acceptably decreased to optimise blood supply whilst maintaining the health of donors [29].

Metabolomics measurements

The levels of 174 metabolites were measured in the Fenland study by the AbsoluteIDQ® Biocrates p180 Kit (Biocrates Life Sciences AG, Innsbruck, Austria) as reported elsewhere in detail

[3231]. We used a Waters Acquity ultra-performance liquid chromatography (UPLC; Waters ltd, Manchester, UK) system coupled to an ABSciex 5500 Qtrap mass spectrometer (Sciex ltd, Warrington, UK). Samples were derivatised and extracted using a Hamilton STAR liquid handling station (Hamilton Robotics Ltd, Birmingham, UK). Flow injection analysis coupled with tandem mass spectrometry (FIA-MS/MS) using multiple reaction monitoring (MRM) in positive mode ionisation was performed to measure the relative levels of acylcarnitines, phosphatidylcholines, lysophosphatidylcholines and sphingolipids. The level of hexose was measured in negative ionisation mode. Ultra-performance liquid chromatography coupled with tandem mass spectrometry using MRM was performed to measure the concentration of amino acids and biogenic amines. The chromatography consisted of a 5-minute gradient starting at 100% aqueous (0.2% Formic acid) increasing to 95% acetonitrile (0.2% Formic acid) over a Waters Acquity UPLC BEH C18 column (2.1 x 50 mm, 1.7 µm, with guard column). Isotopically labelled internal standards are integrated within the Biocrates p180 Kit for quantification. Data was processed in the Biocrates Met*IDQ* software. Raw metabolite readings underwent extensive quality control procedures. Firstly, we excluded from any further analysis metabolites for which the number of measurements below the limit of quantification (LOQ) exceeded 5% of measured samples. Excluded metabolites were carnosine, dopamine, putrescine, asymmetric dimethyl arginine, dihydroxyphenylalanine, nitrotyrosine, spermine, sphingomyelines SM(22:3), SM(26:0), SM(26:1), SM(24:1-OH), phosphatidylcholine acyl-alky 44:4, and phosphatidylcholine diacyl C30:2. Secondly, in samples with detectable but not quantifiable peaks, we assigned random values between 0 and the run-specific LOQ of a given metabolite. Finally, we corrected for batch-effects with a "location-scale" approach, i.e. with normalization for mean and standard deviation of batches.

The levels of up to 38 metabolites were measured in EPIC-Norfolk and INTERVAL using the Metabolon HD4 Discovery platform. Measurements were carried out using MS/MS instruments. For these measurements, instrument variability, determined by calculating the median relative standard deviation, was of 6%. Data Extraction and Compound Identification: raw data was extracted, peak-identified and quality control-processed using Metabolon's hardware and software. Compounds were identified by comparison to library entries of purified standards or recurrent unknown entities. Metabolon maintains a library, based upon authenticated standards, that contains the retention time/index (RI), mass to charge ratio (m/z), and chromatographic data (including MS/MS spectral data) of all molecules present in the library. Identifications were based on three criteria: retention index, accurate mass match to the library +/- 10 ppm, and the MS/MS forward and reverse scores between the experimental data and authentic standards. Metabolite Quantification and Data Normalization: Peaks were quantified using area-under-the-curve. A data normalization step was

performed to correct variation resulting from instrument inter-day tuning differences. Essentially, each compound was corrected in run-day blocks by registering the medians to equal one (1.00) and normalizing each data point proportionately (termed the "block correction").

The levels of 10 metabolites were measured in the INTERVAL study using ^{1}H-NMR spectroscopy[33]. All samples were analysed using a high-throughput serum ^{1}H-NMR metabolomics platform[30]. This provided information on 230 metabolites, including creatinine and several amino acids (alanine, glutamine, glycine, histidine, isoleucine, leucine, valine, phenylalanine, and tyrosine), data on which were used in the present study. Further details of the ^{1}H-NMR spectroscopy, quantification data analysis and identification of the metabolites have been described previously [30,34]. Participants with >30% of metabolite measures missing and duplicated individuals were removed. Metabolite data more than 10 SD from the mean was also removed.

GWAS and meta-analysis

In Fenland and EPIC-Norfolk, metabolite levels were natural log-transformed, winsorised to five standard deviations and then standardised to a mean of 0 and a standard deviation of 1. Genotypes were measured using Affymetrix Axiom or Affymetrix SNP5.0 genotyping arrays. In brief, genotyping in Fenland was done in two waves including 1,500 (Affymetrix SNP5.0) and 9,369 (Affymetrix Axiom) participants (Supplemental table S1) and imputation was done using IMPUTE2 to 1000 Genomes Phase 1v3 (Affymetrix SNP5.0) or phase 3 (Affymetrix Axiom) reference panels (**Supplemental table S1**). In EPIC-Norfolk, 21,044 samples were forwarded to imputation using 1000 Genomes Phase 3 (Oct. 2014) reference panels (**Supplemental table S1**). Imputed SNPs with imputation quality score less than 0.3 or minor allele account less than 2 were removed from the imputed dataset. Genome-wide association analyses were carried out using BOLT-LMM v2.2 adjusting for age, sex, and study-specific covariates in mixed linear models. Alternatively (when the BOLT-LMM algorithm failed) analyses were performed using SNPTEST v2.4.1 in linear regression models, additionally adjusting for the top 4 genetic ancestry principal components and excluding related individuals (defined by proportion identity by descent calculated in Plink[35]) > 0.1875). GWAS analyses in Fenland were performed within genotyping chip, and associations meta-analysed.

In INTERVAL, genotyping was conducting using the Affymetrix Axiom genotyping array. Standard quality control procedures were conducted prior to imputation. The data were phased and imputed to a joint 1000 Genomes Phase 3 (May 2013)-UK10K reference imputation panel. After QC, a total of 40,905 participant remained with data obtained by ^{1}H-NMR spectroscopy. For variants with a MAF of >1% and imputed variants with an info score of >0.4 a univariate GWAS for each of the ten metabolic measures was conducted, after adjustment for technical and seasonal effects,

including age, sex, and the first 10 principal components, and rank-based inverse normal transformation. The association analyses were performed using BOLT-LMM v2.2 and R. Data based on the Metabolon HD4 platform was available for 8,455 participants and SNPTEST v2.5.1 was used to test for associations with metabolite levels adjusting for age, sex, and the first five genetic principle components. In SNPTEST analyses, related individuals (proportion identity by descent > 0.1875) were excluded.

For all GWAS analysis within Fenland, EPIC-Norfolk and INTERVAL, variants with Hardy-Weinberg equilibrium $p<1\times10^{-6}$ and associations with absolute value of effect size >5 or standard error (SE) >10 or <0 were excluded; insertions and deletions were excluded.

For each metabolite, we performed a meta-analysis of z-scores (betas divided by standard errors) as a measure of association, signals and loci (see below), adjusting for genomic control using METAL software. Heterogeneity between studies for each association was estimated by Cochran's Q-test. For each metabolite, we also performed a meta-analysis of beta and standard errors for the subset of studies (Fenland and, when available, EPIC-Norfolk and/or INTERVAL) where we had access to individual level data and standardised phenotype preparation to estimate effect sizes. Quality filters implemented after meta-analysis included exclusion of SNPs not captured by at least 50% of the participating studies and 50% of the maximum sample size for that metabolite and variants with a minor allele frequency below 0.5% percent. As a result, meta-analyses assessed the associations of up to 13.1 million common or low-frequency autosomal SNPs. Chromosome and base pair positions are determined referring to GRCh37 annotation. To define associations between genetic variants and metabolites, we corrected the conventional threshold of genome wide significance for 102 tests (i.e. $p<4.9\text{x}10^{-10}$), corresponding to the number of principal components explaining 95% of the variance of the 174 metabolites, as previously described[36].

Signal selection

For each metabolite, we ranked associated SNPs ($p<4.9\text{x}10^{-10}$) by z-score to select trait-sentinel SNPs and defined an “association” region as the region extending 1 Mb to each side of the trait-sentinel SNP. During forward selection of trait-sentinel SNPs and loci for each trait, adjacent and partially overlapping association regions were merged by extending region boundaries to a further 1 Mb. After defining trait-sentinel SNPs and association regions we defined overall lead-sentinel SNP and loci for any metabolite using a similar approach. Trait-sentinel SNPs were sorted by z-score for the forward selection of lead-sentinel SNPs and a “locus” was defined as the region extending 1 Mb each side of the lead-sentinel SNP. Regions larger than 2 Mb defined in the trait-sentinel association region definition were carried over in the definition of lead-sentinel SNP loci. As a result, all lead-

sentinel SNPs were >1Mb apart from each other and had very low or no linkage disequilibrium (R^2 < 0.05).

For a given locus, independent signals across metabolites were determined based on linkage disequilibrium (LD)-clumping of SNPs that reached the Bonferroni corrected p-value. SNPs with the smallest p-values and an R^2 less than 0.05 were identified as independent signals. LD patterns were estimated with SNP genotype data imputed using the haplotype reference consortium (HRC) reference panel, with additional variants from the combined UK10K plus 1000 Genomes Phase 3 reference panel in the EPIC-Norfolk study (n = 19,254 after removing ancestry outliers and related individuals).

Throughout the manuscript, the term "locus" indicates a genomic region (≥1 Mb each side) of a lead-sentinel SNP harbouring one or more trait-sentinel SNPs; "signal" indicates a group of trait-sentinel SNPs in LD with each other but not with other trait-sentinel SNPs in the locus (R^2 < 0.05); "association" indicates trait-sentinel SNP to metabolite associations defined by a trait-lead SNP and its surrounding region (≥1 Mb each side).

We tested at each locus for conditional independent variants using exact stepwise conditional analysis in the largest Fenland sample (n = 8,714) using SNPTEST v2.5 with the same baseline adjustment as in the discovery approach. To refine signals at those loci we used a more recent imputation for this analysis based on the HRC v1 reference panel and additional SNPs imputed using UK10K and 1000G phase 3. We defined secondary signals as those with a conditional p-value < $5x10^{-8}$. To avoid problems with collinearity we tested after each round if inclusion of a new variant changed associations of all previous variants with the outcome using a joint model. If this model indicated that one or more of the previously selected variants dropped below the applied significance threshold we stopped the procedure, otherwise we repeated this procedure until no further variant met the significance threshold in conditional models. We considered only locus–metabolite associations meeting the GWAS-threshold for significance in the Fenland analysis (n=228).

Colocalisation analyses

For specified loci of interest statistical colocalisation[37] was performed to obtain posterior probabilities (PP) of: H0 – no signal; H1 – signal unique to the metabolite; H2 – signal unique to the trait; H3 – two distinct causal variants in the same locus and H4 – presence of a shared causal variant between a metabolite and a given trait. PP above 80% were considered highly likely. We used p-values and MAFs obtained from the summary statistics with default priors to perform colocalisation.

Hypothesis-free (genetic) assignment of causal genes

To assign likely causal genes to lead SNPs at each locus we generated a scoring system. We identified the nearest gene for each variant by querying HaploReg[38]. Next we integrated expression quantitative trait loci (eQTL) studies (GTEx v6p) to identify genes whose expression levels are associated with metabolite levels using TWAS/FUSION (Transcriptome-wide association study / Functional summary-based imputation)[39]. In doing so, we assigned to each variant-metabolite association one or more associated genes using the variant as common anchor. We further assigned higher impact for a causal gene if either the metabolite variant itself or a proxy in high linkage disequilibrium (R^2>0.8) was a missense variant for a known gene again using the HaploReg database to obtain relevant information. Based on those three criteria we ranked all possible candidate genes and kept those with the highest score as putative causal gene.

Knowledge-based (biological) assignment of causal genes

Metabolite traits are unique among genetically evaluated phenotypes in that the functional characterization of the relevant genes has often already been carried out using classic biochemical techniques. The objective for the knowledge-based assignment strategy was to find the experimental evidence that has previously linked one of the genes proximal to the GWAS lead variant to the relevant metabolite. For many loci and metabolites this 'retrospective' analysis has already been carried out [940].For these cases, previous causal gene assignments were generally adopted. For novel loci, we employed a dual strategy that combined automated database mining with manual curation. In the automated phase, seven approaches were employed to identify potential causal genes among the 20 protein-coding genes closest to each lead variant, as described in detail below, using the shortest distance determined from the lead SNP to each gene's transcription start site (TSS) or transcription end site (TES), with a distance value of 0 assigned if the SNP fell between the TSS and TES.

These 7 approaches were as follows:

1) HMDB metabolite names[41] were compared to each entrez gene name;

2) Metabolite names were compared to the name and synonyms of the protein encoded by each gene[42]

3) HMDB metabolite names and their parent terms (class) were compared to the names for the protein encoded by each gene (UniProt).

4) Metabolite names were compared to rare diseases linked to each gene in OMIM[43] after removing the following non-specific substrings from disease names: uria, emia, deficiency, disease,

transient, neonatal, hyper, hypo, defect, syndrome, familial, autosomal, dominant, recessive, benign, infantile, hereditary, congenital, early-onset, idiopathic;

5) HMDB metabolite names and their parent terms were compared to all GO biological processes associated with each gene after removing the following non-specific substrings from the name of the biological process: metabolic process, metabolism, catabolic process, response to, positive regulation of, negative regulation of, regulation of. For this analysis only gene sets containing fewer than 500 gene annotations were retained.

6) KEGG maps[44] containing the metabolite as defined in HMDB were compared to KEGG maps containing each gene, as defined in KEGG. For this analysis the large "metabolic process" map was omitted.

7) Each proximal gene was compared to the list of known interacting genes as defined in HMDB.

For each text-matching based approach, a fuzzy text similarity metric (pair coefficient) as encoded in the ruby gem "fuzzy_match" was used with a score greater than 0.5 considered as a match.

In the next step, all automated hits at each locus were manually reviewed for plausibility. In addition, other genes at each locus were reviewed if the Entrez gene or UniProt description of the gene suggested it could potentially be related to the metabolite. If existing experimental evidence could be found linking one of the 20 closest genes to the metabolite, that gene was selected as the biologically most likely causal gene. If no clear experimental evidence existed for any of the 20 closest protein coding genes, no causal gene was manually selected. In a few cases multiple genes at a locus had existing experimental evidence. This frequently occurs in the case of paralogs with similar molecule functions. In these cases, all such genes were flagged as likely causal genes.

For each manually selected causal gene, the earliest experimental evidence linking the gene (preferably the human gene) to the metabolite was identified. The median publication year for the identified experimental evidence was 2000.

Enrichment of type 2 diabetes associations among metabolite associated lead variants

We examined whether the set of independent lead metabolite associated variants (N=168) were enriched for associations with type 2 diabetes. We plotted observed versus expected -log10(p values) for the 168 lead variants in a QQ-plot, using association statistics from a type 2 diabetes meta-analysis including 80,983 cases and 842,909 non-cases from the DIAMANTE study [45] (55,005 T2D cases, 400,308 non-cases), UK Biobank[46] (24,758 T2D cases, 424575 non-cases, application number 44448) and the EPIC-Norfolk study (additional T2D cases not included in DIAMANTE study: 1,220 T2D cases and 18,026 non-cases). This QQ-plot was compared to those for 1000 sets of

variants, where variants in each set were matched to the index metabolite variants in terms of MAF, the number of variants in LD (R^2>0.5), gene density and distance to nearest gene (for all parameters +/- 50% of the index variant value), but otherwise randomly sampled from across the autosome excluding the HLA region. MAF and LD parameters for individual variants were determined from the EPIC-Norfolk study (using the combined HRC, UK10K and 1000G imputation as previously described) and gene information was derived from GENCODE v19 annotation[48]. A one-tailed Wilcoxon rank sum test was used to compare the distribution of association –log10 p-values for the metabolite associated variants with that for the randomly sampled, matched, variants.

Functional characterisation of D470N mutant GLP2R

To investigate the functional differences between wild-type (WT) GLP2R and the D470N mutant GLP2R we generated D470N GLP2R mutant constructs using site-directed mutagenesis and characterised canonical GLP2R signalling pathways via cAMP as well as alternative signalling pathways via β-arrestin and P-ERK.

Generation of D470N GLP2R mutant expressing constructs

Human GLP2R cDNA within the pcDNA3.1+ vector was purchased, and Gibson cloning was completed to insert an internal ribosome entry site (IRES) and venus gene downstream of the GLP2R sequence. Following this, QuikChange Lightning site directed mutagenesis was used to perform a single base change from GAC (encoding aspartic acid) to AAC (encoding asparagine) at amino acid position 470 (**Supplemental Figure 2A-B**). Successful mutagenesis was confirmed by DNA Sanger sequencing (**Supplemental Figure 2C**), and the successful products were scaled up for use in functional assays. The WT and mutant GLP2R constructs within the pcDNA3.1+ vector were used to assess signalling by cAMP and P-ERK. To determine β-arrestin recruitment using NanoBiT® technology, an alternative vector was required for lower expression of GLP2R, and fusion of GLP2R to the Large BiT subunit of NanoBiT®. For this, GLP2R was cloned into the pBiT1.1_C[TK/LgBiT] vector using restriction cloning and ligation. DNA Sanger sequencing was then used for confirmation of successful cloning.

Comparison of WT and D470N GLP2R signalling via cAMP

After generation of WT and D470N GLP2R containing constructs, these were used to assess differences in WT and mutant GLP2R signalling. The initial signalling pathway to be assessed was Gαs signalling via cAMP. CHO K1 cells were transiently transfected with WT or mutant GLP2R constructs, then after 16-24 hours were treated with a dose response of GLP-2. cAMP levels were measured following 30 minutes of GLP-2 treatment, in an end-point lysis HitHunter® cAMP assay. The presence of IRES-Venus within the GLP2R expressing vectors allowed transfection efficiency to be determined

for each construct. Transfection efficiency was approximately 60-70%, with no differences between the WT and mutant constructs. Comparison of the GLP-2 dose-response in WT and mutant GLP2R expressing cells revealed no significant differences in signalling, with an almost overlapping dose response curve (Figure 5d).

Comparison of β-arrestin recruitment to the WT and D470N GLP2R

Both β-arrestin 1 and β-arrestin 2 recruitment were assessed using a Nano-Glo® live cell assay in transiently transfected HEK293 cells. Briefly, the recruitment of β-arrestin to GLP2R brings the large and small BiT subunit of NanoBiT® together, resulting in increased luciferase activity. The top concentrations from the GLP-2 dose response in the cAMP assay (1–100 nmol/l GLP-2) were chosen for stimulation of the GLP2R and observation of β-arrestin recruitment. Both β-arrestin 1 and β-arrestin 2 were recruited to the WT GLP2R upon GLP-2 stimulation, in a dose-dependent manner (Supplemental Figure 3a, c). The maximal luciferase activity for both β-arrestin 1 and β-arrestin 2 recruitment to the mutant GLP2R was significantly decreased when compared to the WT GLP2R, indicating the extent of β-arrestin recruitment was markedly decreased (Supplemental Figure 3b, d). The example traces indicate that neither β-arrestin 1 or β-arrestin 2 were recruited to the mutant GLP2R upon stimulation with 1 nmol/l GLP-2, however the same concentration of GLP-2 induced β-arrestin recruitment to the WT GLP2R. Overall there was a significant decrease in β-arrestin 1 and β-arrestin 2 recruitment to the D470N GLP2R mutant (**Figure 5e-f**).

Genetic score and Mendelian randomization analysis for macular telangiectasia type 2

For each metabolite a genetic risk score (GRS) was calculated using all variants meeting genome-wide significance and their beta-estimates as weights obtained from the meta-analysis of studies for which individual level data was available. We used fixed-effect meta-analysis to test for the effect of the GRS on MacTel risk using the summary statistics from the most recent GWAS. A conservative Bonferroni-correction for the number of tested GRS's was used to declare significance ($p<3.5x10^{-4}$). Sensitivity analyses were performed where the pleiotropic *GCKR* variant was removed.

To test for causality between circulating levels of glycine and serine for MacTel we performed two types of Mendelian randomization (MR) analysis. In a two-sample univariable MR[49] we tested for an individual effect of serine (n=4 SNPs) or glycine (n=15 SNPs) on the risk of MacTel using independent non-pleiotropic (i.e. the variant in *GCKR*) genome-wide SNPs as instruments. To this end, we used the inverse variance weighted method to pool SNP ratio estimates using random effects as implemented in the R package *MendelianRandomization.* SNP effects on the risk for MacTel were obtained from[21]. To disentangle the individual effect of those two highly correlated metabolites at the same time we used a multivariable MR model[50] including all SNPs related to

726 serine or glycine (n=15 SNPs). Beta estimates and standard errors for both metabolites and all SNPs
727 were obtained from the summary statistics and mutually used as exposure variables in multivariable
728 MR. Effect estimates were again pooled using a random effect model as implemented in the R
729 package *MendelianRandomization*. This procedure allowed us to obtain causal estimates for both
730 metabolites while accounting for the effect on each other. Estimates can be interpreted as increase
731 in risk for MacTel per 1 SD increase in metabolite levels while holding the other metabolite constant.

732 To estimate a potential clinical usefulness of the identified variants we constructed two
733 GRS's for MacTel using a) sex, the first genetic principal component, and the SNPs rs73171800 and
734 rs9820286 which were identified by the MacTel GWAS study[21] but not found to be related to either
735 glycine or serine in our study and b) all the previous but additionally including genetically predicted
736 serine and glycine at individual levels, via PGS, to the model. An interaction between serine and sex
737 at birth was included to reflect the interaction between SNP rs715 and sex as previously identified [21].
738 To assess the predictive ability of both models, receiver operating characteristic curves were
739 computed based on prediction values in 1,733 controls and 476 MacTel cases.

740 **Identification of genes related to inborn errors of metabolism**

741 Biologically or genetically assigned candidate genes were annotated for IEM association
742 using the Orphanet database[43]. Using a binomial two-tailed test, enrichment of metabolic loci was
743 assessed by comparing the annotated list with the full list of 784 IEM genes in Orphanet against a
744 backdrop of 19,817 protein-coding genes[51]. IEM-annotated loci for which the associated metabolite
745 matched or was closely biochemically related to the IEM corresponding metabolite(s) based on
746 IEMBase[52] were considered further for analysis.

747 We hypothesised that IEM-annotated loci with metabolite-specific consequences could also
748 have phenotypic consequences similar to the IEM. To test this, we first obtained terms describing
749 each IEM and translated them into IEM-related ICD-10 codes using the Human Phenotype Ontology
750 and previously-generated mappings[53,54]. We obtained association statistics from the 85 IEM SNPs for
751 phenotypic associations with corresponding ICD-codes among UK Biobank restricting to diseases
752 with at least 500 cases (N=93, **Fig. 7B,** http://www.nealelab.is/uk-biobank). We tested locus-disease
753 pairs meeting statistical significance (controlling the false discovery rate at 5% to account for
754 multiple testing) for a common genetic signal with the corresponding locus-metabolite association
755 using statistical colocalisation.

756 **Acknowledgement/Funding**

757 M.P. was supported by a fellowship from the German Research Foundation (DFG PI 1446/2-1). C.O.
758 was founded by an early career fellowship at Homerton College, University of Cambridge. L. B. L. W.

759 acknowledges funding by the Wellcome Trust (WT083442AIA). J.G. was supported by grants from
760 the Medical Research Council (MC_UP_A090_1006, MC_PC_13030, MR/P011705/1 and
761 MR/P01836X/1). Work in the Reimann/Gribble laboratories was supported by the Wellcome Trust
762 (106262/Z/14/Z and 106263/Z/14/Z), UK Medical Research Council (MRC_MC_UU_12012/3) and
763 PhD funding for EKB from MedImmune/AstraZeneca. Praveen Surendran is supported by a
764 Rutherford Fund Fellowship from the Medical Research Council grant MR/S003746/1. A. W. is
765 supported by a BHF-Turing Cardiovascular Data Science Award and by the EC-Innovative Medicines
766 Initiative (BigData@Heart). J.D. is funded by the National Institute for Health Research [Senior
767 Investigator Award] [*]. The EPIC-Norfolk study (https://doi.org/10.22025/2019.10.105.00004) has
768 received funding from the Medical Research Council (MR/N003284/1 and MC-UU_12015/1) and
769 Cancer Research UK (C864/A14136). The genetics work in the EPIC-Norfolk study was funded by the
770 Medical Research Council (MC_PC_13048). Metabolite measurements in the EPIC-Norfolk study
771 were supported by the MRC Cambridge Initiative in Metabolic Science (MR/L00002/1) and the
772 Innovative Medicines Initiative Joint Undertaking under EMIF grant agreement no. 115372. We are
773 grateful to all the participants who have been part of the project and to the many members of the
774 study teams at the University of Cambridge who have enabled this research. The Fenland Study is
775 supported by the UK Medical Research Council (MC_UU_12015/1 and MC_PC_13046). Participants
776 in the INTERVAL randomised controlled trial were recruited with the active collaboration of NHS
777 Blood and Transplant England (www.nhsbt.nhs.uk), which has supported field work and other
778 elements of the trial. DNA extraction and genotyping was co-funded by the National Institute for
779 Health Research (NIHR), the NIHR BioResource (http://bioresource.nihr.ac.uk) and the NIHR
780 [Cambridge Biomedical Research Centre at the Cambridge University Hospitals NHS Foundation
781 Trust] [*]. Nightingale Health NMR assays were funded by the European Commission Framework
782 Programme 7 (HEALTH-F2-2012-279233). Metabolon Metabolomics assays were funded by the NIHR
783 BioResource and the National Institute for Health Research [Cambridge Biomedical Research Centre
784 at the Cambridge University Hospitals NHS Foundation Trust] [*]. The academic coordinating centre
785 for INTERVAL was supported by core funding from: NIHR Blood and Transplant Research Unit in
786 Donor Health and Genomics (NIHR BTRU-2014-10024), UK Medical Research Council
787 (MR/L003120/1), British Heart Foundation (SP/09/002; RG/13/13/30194; RG/18/13/33946) and the
788 NIHR [Cambridge Biomedical Research Centre at the Cambridge University Hospitals NHS Foundation
789 Trust] [*].The academic coordinating centre would like to thank blood donor centre staff and blood
790 donors for participating in the INTERVAL trial.

791 This work was supported by Health Data Research UK, which is funded by the UK Medical Research
792 Council, Engineering and Physical Sciences Research Council, Economic and Social Research Council,

Department of Health and Social Care (England), Chief Scientist Office of the Scottish Government Health and Social Care Directorates, Health and Social Care Research and Development Division (Welsh Government), Public Health Agency (Northern Ireland), British Heart Foundation and Wellcome.

*The views expressed are those of the author(s) and not necessarily those of the NHS, the NIHR or the Department of Health and Social Care.

UK Biobank: This research has been conducted using the UK Biobank resource under

Application Number 44448.

Author Contribution

Concept and design: L.A.L. and C.L.

Generation, acquisition, analysis and/or interpretation of data: all authors.

Drafting of the manuscript: L.A.L., M.P., and C.L.

Critical review of the manuscript for important intellectual content and approval of the final version of the manuscript: all authors.

Competing Interests statement

A.S.B. has received grants from AstraZeneca, Biogen, Bioverativ, Merck, Novartis, and Sanofi. J. D. sits on the International Cardiovascular and Metabolic Advisory Board for Novartis (since 2010), the Steering Committee of UK Biobank (since 2011), the MRC International Advisory Group (ING) member, London (since 2013), the MRC High Throughput Science 'Omics Panel Member, London (since 2013), the Scientific Advisory Committee for Sanofi (since 2013), the International Cardiovascular and Metabolism Research and Development Portfolio Committee for Novartis and the Astra Zeneca Genomics Advisory Board (2018).

REFERENCES

1. Wishart, D. S. Metabolomics for investigating physiological and pathophysiological processes. *Physiol. Rev.* **99,** 1819–1875 (2019).
2. Shin, S.-Y. *et al.* An atlas of genetic influences on human blood metabolites. *Nat. Genet.* **46,** 543–550 (2014).
3. Draisma, H. H. M. *et al.* Genome-wide association study identifies novel genetic variants contributing to variation in blood metabolite levels. *Nat. Commun.* **6,** 7208 (2015).
4. Kettunen, J. *et al.* Genome-wide study for circulating metabolites identifies 62 loci and reveals novel systemic effects of LPA. *Nat. Commun.* **7,** 11122 (2016).
5. Illig, T. *et al.* A genome-wide perspective of genetic variation in ... [Nat Genet. 2010] - PubMed result. *Nat. Genet.* **42,** 137–41 (2010).
6. Suhre, K. *et al.* Human metabolic individuality in biomedical and pharmaceutical research. *Nature* **477,** 54–62 (2011).
7. Rhee, E. P. *et al.* A genome-wide association study of the human metabolome in a community-based cohort. *Cell Metab.* **18,** 130–43 (2013).
8. Long, T. *et al.* Whole-genome sequencing identifies common-to-rare variants associated with human blood metabolites. *Nat. Genet.* **49,** 568–578 (2017).
9. Shin, S. Y. *et al.* An atlas of genetic influences on human blood metabolites. *Nat. Genet.* **46,** 543–550 (2014).
10. Draisma, H. H. M. *et al.* Genome-wide association study identifies novel genetic variants contributing to variation in blood metabolite levels. *Nat. Commun.* **6,** 7208 (2015).
11. Astle, W. J. *et al.* The Allelic Landscape of Human Blood Cell Trait Variation and Links to Common Complex Disease. *Cell* **167,** 1415–1429.e19 (2016).
12. Bansal, N. *et al.* Genomic atlas of the human plasma proteome. *Nature* **558,** 73–79 (2018).
13. Learn, D. B., Fried, V. A. & Thomas, E. L. Taurine and hypotaurine content of human leukocytes. *J. Leukoc. Biol.* **48,** 174–182 (1990).
14. Yet, I. *et al.* Genetic Influences on Metabolite Levels: A Comparison across Metabolomic Platforms. *PLoS One* **11,** e0153672 (2016).
15. Lahiri, S. *et al.* Kinetic characterization of mammalian ceramide synthases: Determination of Km values towards sphinganine. *FEBS Lett.* **581,** 5289–5294 (2007).
16. Horowitz, B. *et al.* Asparagine synthetase activity of mouse leukemias. *Science (80-.).* **160,** 533–535 (1968).
17. Babu, E. *et al.* Identification of a Novel System L Amino Acid Transporter Structurally Distinct from Heterodimeric Amino Acid Transporters. *J. Biol. Chem.* **278,** 43838–43845 (2003).
18. Scott, R. A. *et al.* An Expanded Genome-Wide Association Study of Type 2 Diabetes in Europeans. *Diabetes* **66,** 2888–2902 (2017).
19. Fragkos, K. C. & Forbes, A. Citrulline as a marker of intestinal function and absorption in clinical settings: A systematic review and meta-analysis. *United Eur. Gastroenterol. J.* **6,** 181–191 (2018).
20. Estall, J. L., Koehler, J. A., Yusta, B. & Drucker, D. J. The glucagon-like peptide-2 receptor C terminus modulates β-arrestin-2 association but is dispensable for ligand-induced desensitization, endocytosis, and G-protein-dependent effector activation. *J. Biol. Chem.* **280,** 22124–22134 (2005).
21. Scerri, T. S. *et al.* Genome-wide analyses identify common variants associated with macular telangiectasia type 2. *Nat. Genet.* **49,** 559–567 (2017).
22. Gantner, M. L. *et al.* Serine and lipid metabolism in macular disease and peripheral neuropathy. *N. Engl. J. Med.* **381,** 1422–1433 (2019).
23. Garrod, A. E. The incidence of alkaptonuria: a study in chemical individuality. *Lancet* **160,** 1616–1620 (1902).
24. Rath, A. *et al.* Representation of rare diseases in health information systems: The orphanet approach to serve a wide range of end users. *Hum. Mutat.* **33,** 803–808 (2012).

25. Stübiger, G. *et al.* Targeted profiling of atherogenic phospholipids in human plasma and lipoproteins of hyperlipidemic patients using MALDI-QIT-TOF-MS/MS. *Atherosclerosis* **224,** 177–186 (2012).
26. van der Graaf, A., Kastelein, J. J. P. & Wiegman, A. Heterozygous familial hypercholesterolaemia in childhood: Cardiovascular risk prevention. *J. Inherit. Metab. Dis.* **32,** 699 (2009).
27. Lindsay, T. *et al.* Descriptive epidemiology of physical activity energy expenditure in UK adults (The Fenland study). *Int. J. Behav. Nutr. Phys. Act.* **16,** 126 (2019).
28. Day, N. *et al.* EPIC-Norfolk: study design and characteristics of the cohort. European Prospective Investigation of Cancer. *Br. J. Cancer* **80 Suppl 1,** 95–103 (1999).
29. Moore, C. *et al.* The INTERVAL trial to determine whether intervals between blood donations can be safely and acceptably decreased to optimise blood supply: Study protocol for a randomised controlled trial. *Trials* **15,** (2014).
30. Soininen, P. *et al.* High-throughput serum NMR metabonomics for cost-effective holistic studies on systemic metabolism. *Analyst* **134,** 1781–5 (2009).
31. Wittemans, L. B. L. *et al.* Assessing the causal association of glycine with risk of cardio-metabolic diseases. *Nat. Commun.* **10,** (2019).
32. Lotta, L. A. *et al.* Genetic Predisposition to an Impaired Metabolism of the Branched-Chain Amino Acids and Risk of Type 2 Diabetes: A Mendelian Randomisation Analysis. *PLoS Med.* (2016). doi:10.1371/journal.pmed.1002179
33. Di Angelantonio, E. *et al.* Efficiency and safety of varying the frequency of whole blood donation (INTERVAL): a randomised trial of 45 000 donors. *Lancet* **390,** 2360–2371 (2017).
34. Inouye, M. *et al.* Metabonomic, transcriptomic, and genomic variation of a population cohort. *Mol. Syst. Biol.* **6,** 441 (2010).
35. Purcell, S. *et al.* PLINK: A tool set for whole-genome association and population-based linkage analyses. *Am. J. Hum. Genet.* **81,** 559–575 (2007).
36. Li, J. & Ji, L. Adjusting multiple testing in multilocus analyses using the eigenvalues of a correlation matrix. *Heredity (Edinb).* **95,** 221–227 (2005).
37. Giambartolomei, C. *et al.* Bayesian test for colocalisation between pairs of genetic association studies using summary statistics. *PLoS Genet.* **10,** e1004383 (2014).
38. Ward, L. D. & Kellis, M. HaploReg: A resource for exploring chromatin states, conservation, and regulatory motif alterations within sets of genetically linked variants. *Nucleic Acids Res.* **40,** (2012).
39. Gusev, A. *et al.* Integrative approaches for large-scale transcriptome-wide association studies. *Nat. Genet.* **48,** 245–252 (2016).
40. Stacey, D. *et al.* ProGeM: A framework for the prioritization of candidate causal genes at molecular quantitative trait loci. *Nucleic Acids Res.* **47,** (2019).
41. Wishart, D. S. *et al.* HMDB 4.0: The human metabolome database for 2018. *Nucleic Acids Res.* **46,** D608–D617 (2018).
42. Bateman, A. *et al.* UniProt: The universal protein knowledgebase. *Nucleic Acids Res.* **45,** D158–D169 (2017).
43. Rath, A. *et al.* Representation of rare diseases in health information systems: The orphanet approach to serve a wide range of end users. *Hum. Mutat.* **33,** 803–808 (2012).
44. Kanehisa, M., Furumichi, M., Tanabe, M., Sato, Y. & Morishima, K. KEGG: New perspectives on genomes, pathways, diseases and drugs. *Nucleic Acids Res.* **45,** D353–D361 (2017).
45. Mahajan, A. *et al.* Fine-mapping type 2 diabetes loci to single-variant resolution using high-density imputation and islet-specific epigenome maps. *Nat. Genet.* **50,** 1505–1513 (2018).
46. Sudlow, C. *et al.* UK Biobank: An Open Access Resource for Identifying the Causes of a Wide Range of Complex Diseases of Middle and Old Age. *PLoS Med.* **12,** (2015).
47. Collins, R. What makes UK Biobank special? *The Lancet* (2012). doi:10.1016/S0140-6736(12)60404-8

48. Frankish, A. *et al.* GENCODE reference annotation for the human and mouse genomes. *Nucleic Acids Res.* **47,** D766–D773 (2019).
49. Burgess, S., Butterworth, A. & Thompson, S. G. Mendelian randomization analysis with multiple genetic variants using summarized data. *Genet. Epidemiol.* **37,** 658–665 (2013).
50. Burgess, S. & Thompson, S. G. Multivariable Mendelian randomization: The use of pleiotropic genetic variants to estimate causal effects. *Am. J. Epidemiol.* **181,** 251–260 (2015).
51. Harrow, J. *et al.* GENCODE: The reference human genome annotation for the ENCODE project. *Genome Res.* **22,** 1760–1774 (2012).
52. Lee, J. J. Y., Wasserman, W. W., Hoffmann, G. F., Van Karnebeek, C. D. M. & Blau, N. Knowledge base and mini-expert platform for the diagnosis of inborn errors of metabolism. *Genet. Med.* **20,** 151–158 (2018).
53. Köhler, S. *et al.* The human phenotype ontology in 2017. *Nucleic Acids Res.* **45,** D865–D876 (2017).
54. Wu, P. *et al.* Mapping ICD-10 and ICD-10-CM codes to phecodes: Workflow development and initial evaluation. *J. Med. Internet Res.* **21,** (2019).

934 **TABLES**

935

936 **Table 1** Results from Mendelian randomisation (MR) analysis between metabolite levels and risk of
937 macular telangiectasia type 2**.**

938

Metabolite	**Univariable MR**	**Multivariable MR**
Serine (4 SNPs)		
Odds ratio per SD increase	0.06 (0.03; 0.13)	0.10 (0.05; 0.21)
p-value	9.45×10^{-12}	2.95×10^{-9}
Glycine (15 SNPs)		
Odds ratio per SD increase	0.17 (0.08; 0.37)	0.50 (0.29; 0.87)
p-value	9.99×10^{-6}	1.35×10^{-2}

939 MR estimates are based on the inverse variance-weighted method using random effects to pool
940 estimates. All single nucleotide polymorphisms (SNPs) significantly associated with either serine or
941 glycine have been included in multivariable MR analysis. SD = standard deviation

942

943

944 **FIGURE LEGENDS**

945

946 **Figure 1A** Overlap among the 174 plasma metabolites investigated in the present study across three
947 different techniques: Biocrates p180 Kit, Metabolon HD4, and proton nuclear magnetic resonance
948 spectroscopy (NMR). **B** A three-dimensional Manhattan plot displaying chromosomal position (x-
949 axis) of significant associations ($p < 4.9 \times 10^{-10}$, z-axis) across all metabolites (y-axis). Colours indicate
950 metabolite groups. **C** A top view of the 3D-Manhattan plot. Dots indicate significantly associated loci.
951 Colours indicate novelty of metabolite – locus associations. Loci with indication for pleiotropy have
952 been annotated. Barplot on the right-hand side indicates samples sizes for each metabolite
953 comparing the present samples sizes with the previous largest genome-wide association study for a
954 specific metabolite. PCs = phoshpatidylcholines, LysoPCs = lysophophatidylcholines

955

956 **Figure 2A** Distribution of pleiotropy, i.e. number of associated metabolites, among loci identified in
957 the present study. **B** Distribution of polygenicity of metabolites, i.e. number of identified loci for
958 each metabolite under investigation. **C** Scatterplot comparing the estimated heritability of each
959 metabolite against the number of associated loci. Size of the dots indicates samples sizes. **D**
960 Heritability estimates for single metabolites. Colours indicate the proportion of heritability
961 attributed to single nucleotide polymorphisms (SNPs) with large effect sizes ($\beta > 0.25$ per allele). **E –**
962 **M** SNP – metabolite association with indication of non-additive effects. Beta is an estimate from the
963 departure of linearity. **N** Barplot showing the increase in heritability and explained phenotypic
964 variance for each SNP – metabolite pair when including non-additive effects.

965

966 **Figure 3A** Scatterplot comparing the minor allele frequencies (MAF) of associated variants with
967 effect estimates from linear regression models (N loci=499). Colours indicate possible functional
968 consequences of each variant: maroon – nonsynonymous variant; blue – in strong LD ($r^2 > 0.8$) with a
969 nonsynonymous variant and grey otherwise. **B/C** Distribution of effect sizes (B) and allele
970 frequencies (C) based on the type of single nucleotide polymorphism (SNP) (0 – non-coding or
971 synonymous, 1 – in strong LD with nonsynonymous, 2 - nonsynonymous). **D** Distribution of
972 functional annotations of metabolite associated variants (red), trait-associated variants (blue –
973 continuous, purple – diseases) obtained from the GWAS catalogue, and all SNPs included in the
974 present genome-wide association studies. The inlet for exonic variants distinguishes between
975 synonymous (syn) and nonsynonymous variants (nsyn).

Figure 4A Comparison between the genetically prioritized versus biological knowledge-based approaches used in the present study to assign candidate genes to metabolite associated single nucleotide polymorphisms. The Venn-diagram displays the overlap between both approaches. **B** Enrichment of genetically-prioritized genes among biologically plausible or genes linked to inborn errors of metabolism (IEM). **C** Proportion of genetically-prioritized genes encoding for either enzymes or transporters.

Figure 5A Enrichment of associations with type 2 diabetes (T2D: 80,983 cases, 842,909 controls) among metabolite-associated SNPs. Blue dots indicate metabolite-SNPs and grey dots indicate a random selection of matched control SNPs. **B** Opposing $-\log_{10}$(p-values) from the genome-wide association study of plasma citrulline with those from the T2D-GWAS for SNPs located around *GLP2R.* The legend in the upper left gives the posterior probabilities (PP) from statistical colocalisation analysis. H4 = PP for the hypothesis of a shared causal variant. **C** Individual association summary statistics for all citrulline associated SNPs (coded by the citrulline increasing allele) for T2D. **D** GLP-2 dose response curves in cAMP assay for GLP2R wild-type and mutant receptors. The dose response curves of cAMP stimulation by GLP-2 in CHO K1 cells transiently transfected with either GLP2R wild-type or mutant constructs. Data were normalised to the wild-type maximal and minimal response, with 100% being GLP-2 maximal stimulation of the wild-type GLP2R, and 0% being wild-type GLP2R cells with buffer only. Mean ± standard errors are presented (n=4).**E-F** Summary of wild-type and mutant GLP2R beta-arrestin 1 and beta-arrestin 2 responses. Area under the curve (AUC) summary data (n=3-4) displayed for beta-arrestin 1 recruitment (E) and beta-arrestin 2 recruitment (F). AUCs were calculated using the 5 minutes prior to ligand addition as the baseline value. Mean ± standard errors are presented. Normal distribution of log10 transformed data was determined by the D'Agostino & Pearson normality test. Following this statistical significance was assessed by one-way ANOVA with post hoc Bonferroni test. ***p<0.001, *p<0.05. **G** Schematic sketch for the location of the missense variant induces amino acid substitution in the glucagon-like peptide-2 receptor (GLP2R).

Figure 6A Results from polygenic risk scores (PGS) for each metabolite on risk for macular telangiectasia type 2 (MacTel). The dotted line indicates the level of significance after correction for multiple testing. **B** Effect estimates of serine-associated genetic variants on the risk for MacTel. **C** Comparison of effect sizes for lead variants associated with plasma serine levels and the risk for MacTel. **D** Receiver operating characteristic curves (ROC) comparing the discriminative performance

for MacTel using a) sex, the first genetic principal component, and two MacTel varaints (rs73171800 and rs9820286) not associated with metabolite levels (PMID: 28250457), and b) additionally including genetically predicted serine and glycine at individual levels as described in the methods. The area under the curve (AUC) is given in the legend.

Figure 7A Scheme of the workflow to link common variation in genes causing inborn errors of metabolism (IEM) to complex diseases. **7B** Flowchart for the systematic identification of metabolite-associated variants to genes and diseases related to inborn errors of metabolism (IEM). **C** P-values from phenome-wide association studies among UK Biobank using variants mapping to genes knowing to cause IEMs and binary outcomes classified with the ICD-10 code. Colours indicate disease classes. The dotted line indicates the significance threshold controlling the false discovery rate at 5%. **D** Posterior probabilities (PPs) from statistical colocalisation analysis for each significant triplet consisting of a metabolite, a variant, and a ICD-10 code among UK Biobank. The dotted line indicates high likelihood (>80%) for one of the four hypothesis tested: H0 – no signal; H1 – signal unique to the metabolite; H2 – signal unique to the trait; H3 – two distinct causal variants in the same locus and H4 – presence of a shared causal variant between a metabolite and a given trait.